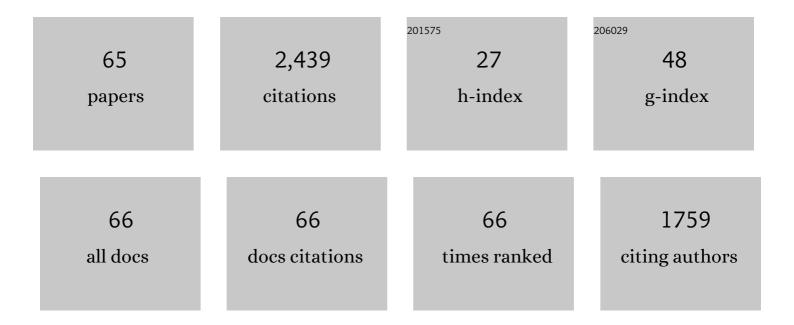
## **Christian Haase**

List of Publications by Year in descending order

Source: https://exaly.com/author-pdf/4854459/publications.pdf

Version: 2024-02-01



#	Article	IF	CITATIONS
1	On the deformation behavior of κ-carbide-free and κ-carbide-containing high-Mn light-weight steel. Acta Materialia, 2017, 122, 332-343.	3.8	153
2	Influence of deformation and annealing twinning on the microstructure and texture evolution of face-centered cubic high-entropy alloys. Acta Materialia, 2018, 150, 88-103.	3.8	151
3	Mechanical properties and deformation behavior of additively manufactured lattice structures of stainless steel. Materials and Design, 2018, 145, 205-217.	3.3	150
4	Combining thermodynamic modeling and 3D printing of elemental powder blends for high-throughput investigation of high-entropy alloys – Towards rapid alloy screening and design. Materials Science & Engineering A: Structural Materials: Properties, Microstructure and Processing, 2017, 688, 180-189.	2.6	145
5	Microstructure evolution and strengthening mechanisms of Fe–23Mn–0.3C–1.5Al TWIP steel during cold rolling. Materials Science & Engineering A: Structural Materials: Properties, Microstructure and Processing, 2014, 617, 52-60.	2.6	112
6	Recrystallization behavior of a high-manganese steel: Experiments and simulations. Acta Materialia, 2015, 100, 155-168.	3.8	96
7	Applying the texture analysis for optimizing thermomechanical treatment of high manganese twinning-induced plasticity steel. Acta Materialia, 2014, 80, 327-340.	3.8	92
8	Grain boundary segregation in Fe–Mn–C twinning-induced plasticity steels studied by correlative electron backscatter diffraction and atom probe tomography. Acta Materialia, 2015, 83, 37-47.	3.8	85
9	Equal-channel angular pressing and annealing of a twinning-induced plasticity steel: Microstructure, texture, and mechanical properties. Acta Materialia, 2016, 107, 239-253.	3.8	71
10	Effect of cold rolling on recrystallization and tensile behavior of a high-Mn steel. Materials Characterization, 2016, 112, 180-187.	1.9	71
11	Identifying Structure–Property Relationships Through DREAM.3D Representative Volume Elements and DAMASK Crystal Plasticity Simulations: An Integrated Computational Materials Engineering Approach. Jom, 2017, 69, 848-855.	0.9	71
12	On the Relation of Microstructure and Texture Evolution in an Austenitic Fe-28Mn-0.28C TWIP Steel During Cold Rolling. Metallurgical and Materials Transactions A: Physical Metallurgy and Materials Science, 2013, 44, 911-922.	1.1	67
13	On the evolution and modelling of brass-type texture in cold-rolled twinning-induced plasticity steel. Acta Materialia, 2014, 70, 259-271.	3.8	66
14	Anisotropic polycrystal plasticity due to microstructural heterogeneity: A multi-scale experimental and numerical study on additively manufactured metallic materials. Acta Materialia, 2020, 185, 340-369.	3.8	64
15	Exploiting Process-Related Advantages of Selective Laser Melting for the Production of High-Manganese Steel. Materials, 2017, 10, 56.	1.3	60
16	Twin-roll strip casting: A competitive alternative for the production of high-manganese steels with advanced mechanical properties. Materials Science & Engineering A: Structural Materials: Properties, Microstructure and Processing, 2015, 627, 72-81.	2.6	53
17	Design of high-manganese steels for additive manufacturing applications with energy-absorption functionality. Materials and Design, 2018, 160, 1250-1264.	3.3	53
18	On the applicability of recovery-annealed Twinning-Induced Plasticity steels: Potential and limitations. Materials Science & Engineering A: Structural Materials: Properties, Microstructure and Processing, 2016, 649, 74-84.	2.6	51

CHRISTIAN HAASE

#	Article	lF	CITATIONS
19	Rapid Alloy Development of Extremely High-Alloyed Metals Using Powder Blends in Laser Powder Bed Fusion. Materials, 2019, 12, 1706.	1.3	49
20	Structural/textural changes and strengthening of an advanced high-Mn steel subjected to cold rolling. Materials Science & Engineering A: Structural Materials: Properties, Microstructure and Processing, 2016, 651, 763-773.	2.6	46
21	Enhancement of the strength-ductility combination of twinning-induced/transformation-induced plasticity steels by reversion annealing. Materials Science & Engineering A: Structural Materials: Properties, Microstructure and Processing, 2017, 681, 56-64.	2.6	46
22	Tailoring the Mechanical Properties of a Twinning-Induced Plasticity Steel by Retention of Deformation Twins During Heat Treatment. Metallurgical and Materials Transactions A: Physical Metallurgy and Materials Science, 2013, 44, 4445-4449.	1.1	41
23	Strain-Rate-Dependent Deformation Behavior and Mechanical Properties of a Multi-Phase Medium-Manganese Steel. Metals, 2019, 9, 344.	1.0	37
24	Production of Ti–6Al–4V billet through compaction of blended elemental powders by equal-channel angular pressing. Materials Science & Engineering A: Structural Materials: Properties, Microstructure and Processing, 2012, 550, 263-272.	2.6	35
25	Defect formation and prevention in directed energy deposition of high-manganese steels and the effect on mechanical properties. Materials Science & amp; Engineering A: Structural Materials: Properties, Microstructure and Processing, 2020, 772, 138688.	2.6	34
26	Microstructure Evolution of Binary and Multicomponent Manganese Steels During Selective Laser Melting: Phase-Field Modeling and Experimental Validation. Metallurgical and Materials Transactions A: Physical Metallurgy and Materials Science, 2019, 50, 2022-2040.	1.1	33
27	Revealing the relation between microstructural heterogeneities and local mechanical properties of complex-phase steel by correlative electron microscopy and nanoindentation characterization. Materials and Design, 2021, 203, 109620.	3.3	33
28	Optimal Design for Metal Additive Manufacturing: An Integrated Computational Materials Engineering (ICME) Approach. Jom, 2020, 72, 1092-1104.	0.9	32
29	Understanding the process-microstructure correlations for tailoring the mechanical properties of L-PBF produced austenitic advanced high strength steel. Additive Manufacturing, 2019, 30, 100914.	1.7	31
30	Effects of process parameters on bead shape, microstructure, and mechanical properties in wire + arc additive manufacturing of Al0.1CoCrFeNi high-entropy alloy. Journal of Manufacturing Processes, 2021, 68, 1314-1327.	2.8	30
31	Texture Evolution of a Cold-Rolled Fe-28Mn-0.28C TWIP Steel during Recrystallization. Materials Science Forum, 2013, 753, 213-216.	0.3	26
32	Microstructure and texture evolution of a high manganese TWIP steel during cryo-rolling. Materials Characterization, 2017, 132, 20-30.	1.9	26
33	Combined deformation twinning and short-range ordering causes serrated flow in high-manganese steels. Materials Science & Engineering A: Structural Materials: Properties, Microstructure and Processing, 2019, 746, 434-442.	2.6	26
34	Enhanced precipitation strengthening of multi-principal element alloys by $\hat{I}^{2}$ - and B2-phases. Materials and Design, 2021, 198, 109315.	3.3	19
35	Improving sinterability of Ti–6Al–4V from blended elemental powders through equal channel angular pressing. Materials Science & Engineering A: Structural Materials: Properties, Microstructure and Processing, 2013, 565, 396-404.	2.6	18
36	Combined Al and C alloying enables mechanism-oriented design of multi-principal element alloys: Ab initio calculations and experiments. Scripta Materialia, 2020, 178, 366-371.	2.6	18

CHRISTIAN HAASE

#	Article	IF	CITATIONS
37	Combined κ-carbide precipitation and recovery enables ultra-high strength and ductility in light-weight steels. Materials Science & Engineering A: Structural Materials: Properties, Microstructure and Processing, 2020, 795, 139928.	2.6	18
38	The microstructural effects on the mechanical response of polycrystals: A comparative experimental-numerical study on conventionally and additively manufactured metallic materials. International Journal of Plasticity, 2021, 140, 102941.	4.1	18
39	Controlling microstructure and mechanical properties of additively manufactured high-strength steels by tailored solidification. Additive Manufacturing, 2020, 35, 101389.	1.7	16
40	Influence of rolling asymmetry on the microstructure, texture and mechanical behavior of high-manganese twinning-induced plasticity steel. Materials Science & Engineering A: Structural Materials: Properties, Microstructure and Processing, 2018, 709, 172-180.	2.6	15
41	Correlation of defect density with texture evolution during cold rolling of a Twinning-Induced Plasticity (TWIP) steel. Materials Science & Engineering A: Structural Materials: Properties, Microstructure and Processing, 2018, 711, 69-77.	2.6	15
42	Mechanical twinning and texture evolution during asymmetric warm rolling of a high manganese steel. Materials Science & Engineering A: Structural Materials: Properties, Microstructure and Processing, 2019, 764, 138183.	2.6	15
43	The Influence of Warm Rolling on Microstructure and Deformation Behavior of High Manganese Steels. Metals, 2019, 9, 797.	1.0	15
44	On the influence of ϰ-carbides on the low-cycle fatigue behavior of high-Mn light-weight steels. International Journal of Fatigue, 2021, 150, 106327.	2.8	14
45	Compositional heterogeneity in multiphase steels: Characterization and influence on local properties. Materials Science & Engineering A: Structural Materials: Properties, Microstructure and Processing, 2021, 827, 142078.	2.6	14
46	From High-Manganese Steels to Advanced High-Entropy Alloys. Metals, 2019, 9, 726.	1.0	11
47	AixViPMaP®—an Operational Platform for Microstructure Modeling Workflows. Integrating Materials and Manufacturing Innovation, 2019, 8, 122-143.	1.2	11
48	Tailoring the nanostructure of laser powder bed fusion additively manufactured maraging steel. Additive Manufacturing, 2020, 36, 101561.	1.7	11
49	Application of Texture Analysis for Optimizing Thermo-Mechanical Treatment of a High Mn TWIP Steel. Advanced Materials Research, 0, 922, 213-218.	0.3	10
50	Directed energy deposition of Inconel 718 powder, cold and hot wire using a six-beam direct diode laser set-up. Additive Manufacturing, 2021, 47, 102269.	1.7	10
51	Modeling the Effect of Primary and Secondary Twinning on Texture Evolution during Severe Plastic Deformation of a Twinning-Induced Plasticity Steel. Materials, 2018, 11, 863.	1.3	9
52	Physical Metallurgy of High Manganese Steels. Metals, 2019, 9, 1053.	1.0	9
53	Thermo-micro-mechanical simulation of metal forming processes. International Journal of Solids and Structures, 2019, 178-179, 59-80.	1.3	9
54	Precise control of microstructure and mechanical properties of additively manufactured steels using elemental carbon powder. Materials Letters, 2021, 295, 129788.	1.3	6

CHRISTIAN HAASE

#	Article	IF	CITATIONS
55	Comparative Study of the Influence of Reversion―and Recovery―Annealing on the Mechanical Behavior of Highâ€Manganese Steels with Varying Stacking Fault Energy. Steel Research International, 2018, 89, 1700377.	1.0	5
56	Metallurgical Gradients in Structural Materials: Potential and Challenges in Creating Artificial Segregations in Medium Manganese Steel via Rollâ€Bonding. Steel Research International, 0, , 2100429.	1.0	5
57	Microstructure and Texture Evolution during Recrystallization of a Fe-Mn-C Alloy. Materials Science Forum, 2013, 753, 177-180.	0.3	4
58	Computer-Aided Material Design for Crash Boxes Made of High Manganese Steels. Metals, 2019, 9, 772.	1.0	3
59	Correlating the microstructural heterogeneity with local formability of coldâ€rolled DP and CP steels through hardness gradients. Steel Research International, 0, , .	1.0	2
60	Ti-6Al-4V Billet Produced by Compaction of BE Powders Using Equal-Channel Angular Pressing. Key Engineering Materials, 0, 520, 301-308.	0.4	1
61	Development of Fine-Grained High-Mn Steelby Cold Rolling and Annealing. Materials Science Forum, 0, 838-839, 434-439.	0.3	1
62	Deformation and Recrystallization Textures in a High-Mn Steel Subjected to Large Strain Cold Rolling. , 2016, , 147-152.		1
63	Deformation and Recrystallization Textures in A High-Mn Steel Subjected to Large Strain Cold Rolling. , 0, , 147-152.		0
64	Recrystallization kinetics and texture evolution during annealing of cold-rolled high-Mn steel. AIP Conference Proceedings, 2017, , .	0.3	0
65	Phase-Field Modeling of Microstructure Evolution of Binary and Multicomponent Alloys During Selective Laser Melting (SLM) Process. Minerals, Metals and Materials Series, 2019, , 301-309.	0.3	Ο